PAPER

Spontaneous electrification of fluoropolymer–water interfaces probed by electrowetting†

Arun G. Banpurkar,*[ab] Yogesh Sawane,[a] Sandip M. Wadhai,[ab]
C. U. Murade,[b] Igor Siretanu,[b] D. van den Ende[b] and F. Mugele [iD] [b]

Fluoropolymers are widely used as coatings for their robustness, water-repellence, and chemical inertness. In contact with water, they are known to assume a negative surface charge, which is commonly attributed to adsorbed hydroxyl ions. Here, we demonstrate that a small fraction of these ions permanently sticks to surfaces of Teflon AF and Cytop, two of the most common fluoropolymer materials, upon prolonged exposure to water. Electrowetting measurements carried out after aging in water are used to quantify the density of 'trapped' charge. Values up to -0.07 and -0.2 mC m^{-2} are found for Teflon AF and for Cytop, respectively, at elevated pH. A similar charge trapping process is also observed upon aging in various non-aqueous polar liquids and in humid air. A careful analysis highlights the complementary nature of electrowetting and streaming potential measurements in quantifying interfacial energy and charge density. We discuss the possible mechanism of charge trapping and highlight the relevance of molecular scale processes for the long term stability and performance of fluoropolymer materials for applications in electrowetting and elsewhere.

1. Introduction

Amorphous fluoropolymers are chemically very resistive and inert. They are hydrophobic and optically transparent and they possess a low dielectric constant. As a result, they are widely applied as coating materials to protect all sorts of surfaces in the semiconductor industry, optical devices, and biomedical applications from harsh environments.[1] Two representatives of these materials, Teflon AF and Cytop, are also the most popular materials for the fabrication of hydrophobic dielectric layers with excellent smoothness and chemical and topographic homogeneity for electrowetting (EW) 'on dielectric' experiments.[2] The EW effect

[a]Center for Advanced Studies in Materials Science and Condensed Matter Physics, Department of Physics, University of Pune, Pune-411 007, India. E-mail: agb@physics.unipune.ac.in

[b]Physics of Complex Fluids, Faculty of Science and Technology, MESA$^+$ Institutes, University of Twente, P. O. Box 217, 7500AE Enschede, The Netherlands

† Electronic supplementary information (ESI) available. See DOI: 10.1039/c6fd00245e

relies on the reversible charging and discharging of the interface between a conductive polar phase, frequently an aqueous electrolyte, and the dielectric layer upon applying an external bias voltage between the liquid and one or more electrodes submerged under the dielectric layer. Ideally, the reduction of the contact angle θ upon applying a voltage U is described by the so-called EW equation[2]

$$\cos \theta(U) = \cos \theta_Y + \eta \qquad (1)$$

here, θ_Y is Young's contact angle and $\eta = c_d U^2/2\gamma$ is the dimensionless EW number. This equation measures the ratio between the electrostatic energy per unit area of the parallel plate capacitor with capacitance c_d that is formed by the liquid, the dielectric layer and the submerged electrode on the substrate and the surface tension γ of the drop. In practice, deviations from this ideal behavior are routinely observed. The most notable deviation is the phenomenon of contact angle saturation, which subsumes probably a variety of microscopic processes that prevent the contact angle from decreasing below a certain system specific minimum 'saturation' angle θ_s.[3,4] For voltages beyond the corresponding value of η_s, θ ceases to decrease. While the overall behavior at lower voltage typically follows the EW equation rather well, a detailed analysis of the EW response still reveals deviations, even for $\eta < 0.5$, in particular in cases of DC voltage. The contact angle variation has been reported to depend on the polarity of the applied voltage,[5–8] sometimes the maximum contact angle was found at non-zero bias voltage,[8–11] and EW response curves were reported to depend on the pH (ref. 5) of the aqueous phase and on the types of ions dissolved.[12] Some of these aspects were reproduced in simulations that display a field-dependent specific adsorption of certain types of ions.[13] Many of these studies date back to the early 2000s when researchers were looking for optimum materials. In the meantime, a certain degree of convergence regarding materials choices, fabrication procedures, and operating conditions lead to reasonably stable systems in many cases. Yet, these choices have largely been based on empirical tests, rather than systematic attempts to address the underlying physico-chemical phenomena at the relevant solid–liquid and liquid–liquid interfaces. Perhaps as a consequence of this situation, the long term stability of devices such as EW displays, optofluidic lenses, energy harvesting systems, *etc.* still suffers from the poorly understood physical chemistry of the relevant solid–liquid and liquid–liquid interfaces.

Except for a few remarks and one systematic study by Quinn *et al.*,[5] little connection has been made between EW performance and the general charging properties of the electric double layer (EDL) at hydrophobic–water interfaces. The latter have been widely studied in physical chemistry for decades (for some reviews, see *e.g.*[14–16]) because of, amongst other reasons, the importance of hydrophobic interactions in biological self-assembly processes such as protein folding and the formation of lipid bilayers.[17] A large body of electrokinetic studies demonstrate that hydrophobic–water interfaces very generally display a negative surface charge that increases strongly with increasing pH. *Vice versa* the interfaces typically reach an isoelectric point at pH values somewhere between 2 and 4. This behavior holds rather universally for non-polar hydrophobic polymer surfaces, for hydrophobic self-assembled monolayers, and also for oil–water interfaces as well as water–air interfaces, where air behaves as a 'hydrophobic' material that cannot

participate in hydrogen bonding. It is widely believed that the negative charge is caused by the preferential adsorption of hydroxyl ions (OH^-).[14,15,18–20] They accommodate the loss of hydrogen bonding that is imposed by the presence of the inert hydrophobic surface. While this scenario is consistent with the strong pH-dependence and the weak dependence on added salt in titration measurements, the details of the charging mechanism, in particular in the presence of specifically adsorbing ions,[21] are very complex and still heavily debated. Some recent spectroscopic results even question the basic scenario of OH^- adsorption.[22]

Recently, a series of phenomena and applications have been reported that combine aspects of macroscopic electrowetting and the microscopic physical chemistry of solid–electrolyte interfaces. Examples include the spontaneous charging of drops ejected from pipettes,[23] energy harvesting systems based on reverse electrowetting and modulation of the area of electric double layers,[24,25] dielectric-free electrowetting on graphite surfaces[26] as well as ion-adsorption induced wetting transitions in oil–water–mineral surfaces.[27]

In the present work, we analyze another striking phenomenon that has been reported but not systematically addressed in the literature,[5,11,28] namely the spontaneous accumulation of permanently trapped charge at fluoropolymer surfaces upon prolonged exposure to water, as sketched in Fig. 1. EW response curves recorded after aging in water display a pronounced asymmetry between positive and negative bias voltage that increases with increasing aging time and with pH. From this asymmetry a small but finite density of permanently trapped negative charge carriers is extracted. In contrast, the charge density determined from complementary streaming potential measurements is independent of the aging time, yet it displays the same characteristic increase with increasing pH. Our analysis rationalizes these observations by analyzing the different sensitivities of the two techniques for interfacial charge density and for interfacial energy and thereby highlights an important relation between microscopic physical chemistry and macroscopic wettability at hydrophobic–water interfaces.
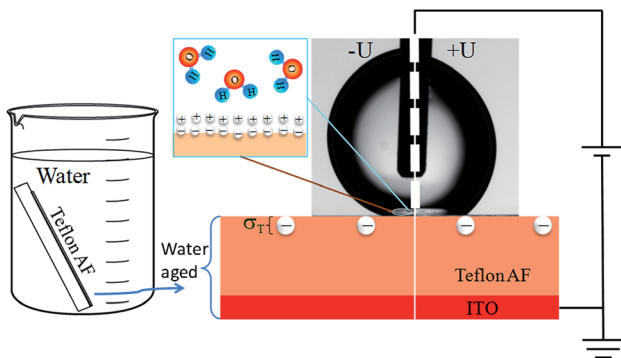

Fig. 1 Illustration of the experiments. Left: Aging of fluoropolymer surfaces in water. Right: Electrowetting response is recorded subsequently in an ambient oil environment. The split image highlights the difference between negative (left) and positive (right) polarity. All voltages throughout this work are reported with respect to the grounded ITO electrode on the substrate.

The work is organized as follows. Section 2 provides all relevant information about materials and experimental protocols used in this study. Section 3 describes the phenomena observed in the EW experiments and their analysis along the lines of the original work by Verheijen and Prins.[29] In Section 4, we present the results of the streaming potential measurements. Finally, we provide in Section 5 a simple model that reconciles the apparent contradiction between EW and streaming potential measurements. We discuss aspects of a potential microscopic mechanism of charge trapping and some consequences of our observations for the durability and degradation of fluorinated polymer–water interfaces in EW applications.

2. Methods and materials

Dielectric films

Two types of hydrophobic fluoropolymers were used in this study, Teflon AF 1600 (DuPont) and Cytop (Asahi, glass). Both materials were purchased as solutions in fluorinated solvents. Fluoropolymer films with a thickness of 3–5 μm were deposited onto ITO (indium-tin-oxide)-covered glass slides using dip coating following a procedure adopted from ref. 6 and 30: ITO glass substrates (Präzisions Glas & Optik, Germany, with 25 nm ITO) were cleaned in an ultrasound bath using a diluted surfactant solution (Mucasol®), sonicated in Millipore water, acetone, and ethanol and were finally rinsed in reagent grade iso-propanol. Substrates were dried under a filtered nitrogen gas flow and stored in a laminar flow cabinet. Teflon AF 1600 solution (6 wt% in Fluorinert® FC40, Sigma) was used for the coating at an immersion/withdrawal speed of 15 cm min^{-1}. This layer was dried under a laminar air flow and thermally cured for 10 min in a vacuum oven at 110 °C. The procedure was repeated once to reach the desired dielectric thickness. Finally, substrates were thermally cured at 160 °C for 10 min and at 240 °C for 30 min in a vacuum oven for the complete removal of any residual solvent and annealing above the glass transition temperature. Cytop® films were prepared by the same procedure. Immediately after the final annealing step, the samples were transferred to a glove box with dry nitrogen and stored there. Such samples are henceforth referred to as pristine substrates.

Water exposure

Pristine substrates were exposed to water (and in a few exploratory experiments to ethylene glycol, acetone, ethanol, isopropyl alcohol – all purchased from Sigma Aldrich and used without further treatment) by immersing them for controlled waiting times t_w of between a few minutes and up to 120 h into a beaker containing the liquid. De-ionized water (Millipore; Synergic UV; conductivity: 0.055 μS cm^{-1}) was used and the pH was adjusted by adding stock solutions of HCl (Fluka 99.9%) and NaOH (Fluka 99.9%). In a few test experiments, KCl was added to increase the conductivity to levels between 5 and 27 mS cm^{-1}. At the end of the exposure the substrates were taken out of the beaker and dried in a dry nitrogen gas jet for 10 min and immediately characterized using either electrowetting or streaming potential measurements. In a few cases, we also explored exposure of the samples to air of increased humidity. In these cases, the pristine substrates were stored in a sealed container with 98% relative humidity for 30 h. Note that no

external voltage was applied to any of the samples during any of the aging procedures.

Electrowetting

Electrical connections to the ITO electrode were established after aging in water by gluing copper wires to the electrode using conductive silver paste. Subsequently, the samples were placed in a glass-cuvette ($40 \times 40 \times 40$ mm^3) filled with silicone oil (viscosity $\mu = 5$ cSt, density $\rho = 1.1$ g cm^{-3}, Sigma-Aldrich). Saline water with a conductivity 3.0 mS cm^{-1} was prepared by adding a suitable amount of KCl salt in Millipore water (control experiments with salt concentrations between zero and 20 mM did not reveal any salt-dependence of the results, as expected). A 5 µL drop of that solution was gently pipetted onto the sample surface and electrically connected using a thin platinum wire. The Young's angle for pristine samples under oil was $\theta_Y = 167 \pm 1°$. A triangular voltage ramp with ramping times varying between 25 s and 1000 s was generated with a frequency generator (Agilent 33220A) and amplified to the desired voltage level using a high voltage amplifier (PZD700A; Trek, USA). The voltage was applied between the drop and the ITO electrode on the sample, as illustrated in Fig. 1. The potential of the ITO electrode is used as common ground throughout this work. EW response curves in ambient oil were recorded for at least 100 voltage cycles on each sample. The corresponding contact angle, $\theta(U)$ was recorded using an Optical Contact Angle goniometer, OCA-15$^+$, and analyzed using the SCA-20 software (both from Dataphysics GmbH, Germany). The capacitance per unit area c of the dielectric layer was estimated from the values of its dielectric constant, $\varepsilon = 1.98$,[29] and thicknesses, $d = 3...4$ µm, as determined by a profilometer. The EW response curves were analyzed by fitting them with a modified electrowetting equation for the voltage-dependent contact angle $\theta(U)$

$$\cos \theta(U) = \cos \theta_Y + \frac{c}{2\gamma}(U - U_T)^2 \qquad (2)$$

that includes a finite 'trapping voltage' U_T to account for a possible asymmetric response to positive and negative bias voltages. $\gamma = 39$ mJ m^{-2} is the tension of the oil–water interface. c was determined for each sample independently by fitting to eqn (2). Typical values varied between 3 and 4 µF m^{-2}, in reasonable agreement with the profilometer measurements.

Streaming potential measurements

Streaming potential measurements to determine the ζ potential and thereby the surface charge density σ_s of the diffuse layer were carried out using a ZetaCAD instrument (CAD instruments, France). To this end, two Teflon coated substrates of size 1×1.9 cm^2 were mounted at a distance of 100 µm from each other as top and bottom walls in a rectangular flow-cell. The streaming potential U_s was measured as a function of the pressure difference ΔP across the flow cell. U_s was found to be linear in ΔP as expected. The ζ potential was extracted from U_s using the standard Smoluchowski formula $\zeta = \dfrac{U_s \mu k_L}{\varepsilon_w \varepsilon_0 \Delta P}$. Here $\varepsilon_0 \varepsilon_w$ is permittivity, μ the viscosity and k_L the conductivity of the solution.[31] Streaming potential measurements were performed at variable pH. The finite stabilization time of the

streaming potential signal after each change of the applied pressure limited the time resolution of the ζ potential measurement to approximately 1 h.

All annealing procedures as well as the subsequent characterization experiments were carried out at a room temperature of approx. 22 °C.

3.   Electrowetting experiments

Charge trapping on Teflon AF films aged in water

Fig. 2 shows the contact angles as a function of time while continuously varying the voltage from −80 V to +80 V in a triangular manner (red line). Initial tests demonstrated that the ramping time did not have any substantial effect within a range of 25 s and 1000 s (see ESI Fig. S1†). The majority of the experiments were therefore carried out with relatively short ramping times of 1 min or less. Pristine samples displayed an almost symmetric response for positive and negative polarity. Samples that were aged in water for several hours prior to the EW experiments, however, displayed an increasingly asymmetric response, with stronger contact angle reductions for positive bias voltage on the drop. For Cytop samples, the asymmetry is typically more pronounced than for Teflon AF. In some cases, the asymmetry can be so pronounced that the contact angle can increase rather substantially depending on the polarity of the applied voltage, see Fig. 2b. This phenomenon has been denoted as 'electrodewetting' in the literature. It arises rather naturally in cases of an asymmetric EW response.

Fig. 3 shows one voltage cycle for each of the same three sample ages as in Fig. 2, represented in the more common form of $\cos \theta$ *versus* the applied voltage. The data clearly show how the apex of the EW curves shift towards negative voltages with increasing aging time in water prior to the measurement. Note that Young's angle also decreases by a few degrees with increasing sample age along with the (much more dramatic) shift of the apex of the EW curves.

Systematic experiments were performed for a larger range of aging times. For each case, the EW curves were fitted using eqn (2) and the trapping voltage U_T was extracted. As shown in Fig. 4a, U_T increased from a few volts after a minimum exposure of 15 min to ≈ -22 V after 24 h. Little variation beyond this saturation
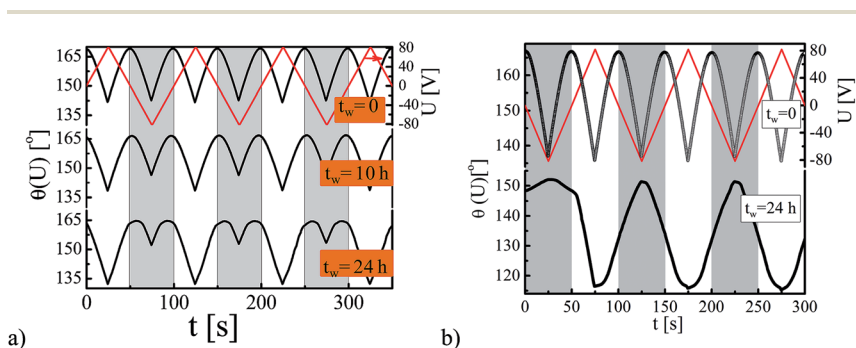

Fig. 2 Contact angle of water in oil (black lines) *vs.* time over several cycles of a triangular waveform for three Teflon AF samples (a) and two Cytop samples (b) after aging in deionized water at pH ≈ 6 for various waiting times as indicated. Grey regions correspond to negative and white ones to positive bias on the drop. Red line: applied voltage *vs.* time. Voltage ramping rate: 1.4 V s^{-1}.
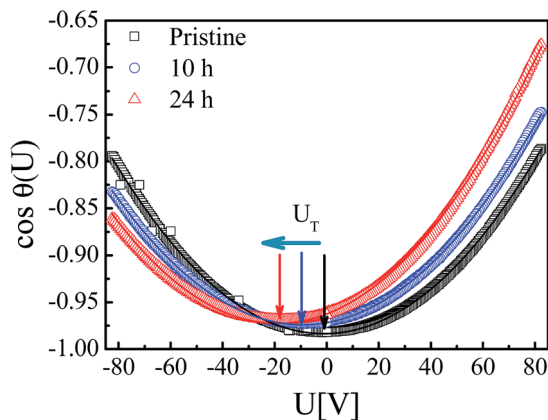
Fig. 3 Electrowetting response curves for Teflon AF pristine ($\square$) and $t_w = 10$ h ($\circ$) and $t_w = 24$ h ($\triangle$) aged surfaces. Solid lines: Young−Lippmann fit (eqn (2)) to the experimental data points. The arrow indicates increasing t_w.
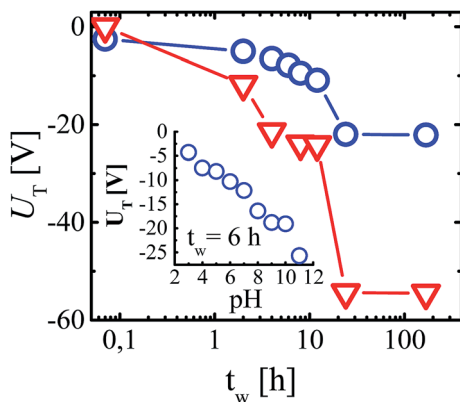

Fig. 4 Trapping voltage *vs.* aging time in water at pH 6 (main panel) for Teflon AF (blue circles) and Cytop (red triangles). Inset: U_T *vs.* pH for Teflon AF at $t_w = 6$ h.

was observed for waiting times up to 160 h, suggesting that the surface reached an equilibrium configuration after approximately 24 h. An additional series of experiments with aging solutions of variable pH showed that the trapping voltage becomes increasingly negative with increasing pH, see inset Fig. 4. At pH 3, the lowest pH investigated, the EW response curves remained almost symmetric throughout the aging process (note that the pH-dependent measurements were performed at a fixed waiting time of $t_w = 6$ h, therefore the absolute values of U_T do not reflect the final equilibrium values).

Robustness and universality of charge trapping

We interpret the increasing asymmetry of the EW response as a consequence of the trapping of (negative) charge carriers at the solid–liquid interface during the aging process. Before discussing this interpretation in more detail, we report

a few additional aspects and control experiments. First of all, we note that the observations described here are very robust. While the absolute values of the contact angles and their variation with applied voltage vary by a few degrees between experiments carried out over an extended period of more than one year in the laboratories at the University of Twente (The Netherlands) and Univ. of Pune (India), the general trend of an increasingly negative trapping voltage with increasing time were reproduced for several tens of samples.

Interestingly, exploratory experiments with other liquids demonstrated that the accumulation of charge at the fluoropolymer surface is not unique to water as a liquid medium. Similar asymmetries in the EW response curves were found for Teflon AF films that were aged in ethylene glycol, acetone, ethanol and isopropyl alcohol. Only the degree of charge varied between the different fluids, as qualitatively illustrated in Fig. 5. Perhaps even more remarkably, spontaneous electrification – albeit to a somewhat lesser extent – was also observed upon exposing Teflon AF for an extended time to nearly water–saturated air, see Fig. S3.†

To complement the aging experiments in pure fluid in the absence of any applied bias voltage, we also performed a few control experiments while applying a voltage. Those experiments were performed by immersing pristine Teflon AF samples in silicone oil, as in all of the EW measurements described above. EW curves were recorded while continuously ramping up and down the voltage applied to water drops of unadjusted pH (≈ 6) without added salt (see Fig. 6). At short times, the data display the usual weak asymmetry between positive and negative bias. Upon extended exposure to the fluid and the applied voltage,
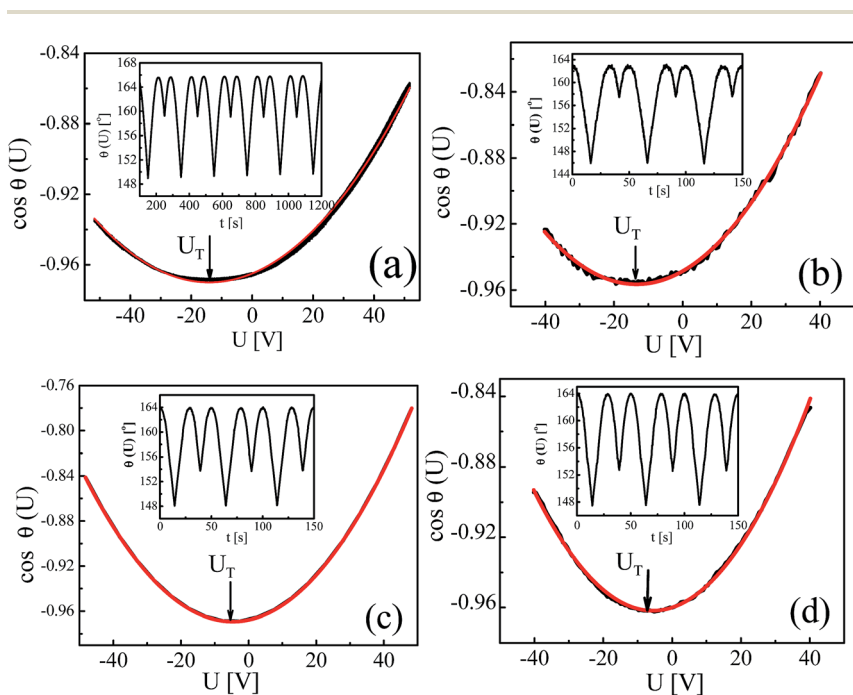

Fig. 5 Electrowetting response curves for Teflon AF aged in various polar fluids. (a) Ethylene glycol for $t_w = 48$ h, (b) acetone for $t_w = 8$ h, (c) ethanol for $t_w = 8$ h and (d) isopropyl alcohol for $t_w = 8$. Insets: contact angle $vs.$ time for a few voltage cycles.

however, the asymmetry grows as illustrated by the two solid lines $\theta(-U)$ and $\theta(+U)$ that trace the contact angles measured for maximum negative and positive drop voltage, respectively. Note that the maximum contact angle also slightly decreases with increasing time, similar to the observations for samples aged without bias voltage (see Fig. 2 and 3).

Suspecting that the increasing asymmetry of the EW response curves is caused by permanent adsorption of charge carriers, we changed the profile of the applied voltage ramps to compare the results upon aging the samples under positive or negative bias separately. Fig. 7a and b show EW response curves for initially pristine surfaces that are aged while continuously applying voltage ramps between zero and +52 V in (a) and −52 V in (b). Clearly, the aging behavior is very different. Only a minor relaxation is observed for positive bias voltages on the drop, *i.e.* for conditions that cations are pulled towards the Teflon surface, whereas a substantial degradation is observed in the case of negative bias on the drop, *i.e.* when pulling anions toward the solid surface. Repelling anions from the Teflon–water interface thus suppresses the aging process.

Interpretation: charge trapping at solid–liquid interface

We interpret the results shown here as a consequence of permanent trapping of charge carriers at the fluoropolymer surface. To quantify the amount of trapped charge, we adopt the model proposed by Prins and Verheijen. The key idea of the model is that ions from the solution are permanently trapped at the solid–liquid interface or at some distance δ below the interface, as sketched in Fig. 8. For the sake of completeness, we provide the derivation of the model in the appendix of this work. A few aspects from this derivation are crucial for the interpretation of the values of U_T. First of all, the result of the energy minimization of the drop yields the expression given in eqn (2) for the equilibrium contact angle. Second, the equation yields the relation

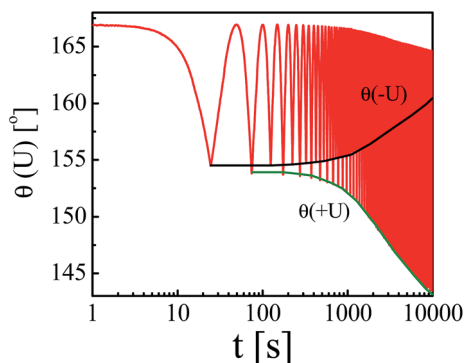$$\sigma_T = \frac{\varepsilon\varepsilon_0}{d - \delta} U_T \tag{3}$$

Fig. 6 Contact angle *vs.* time for continuously ramped DC voltage on an initially pristine Teflon AF surface. Black solid lines trace the minimum contact angles for maximum positive and negative voltage as indicated. Voltage ramping rate: $dU/dt = 2$ V s^{-1}. pH = 6.
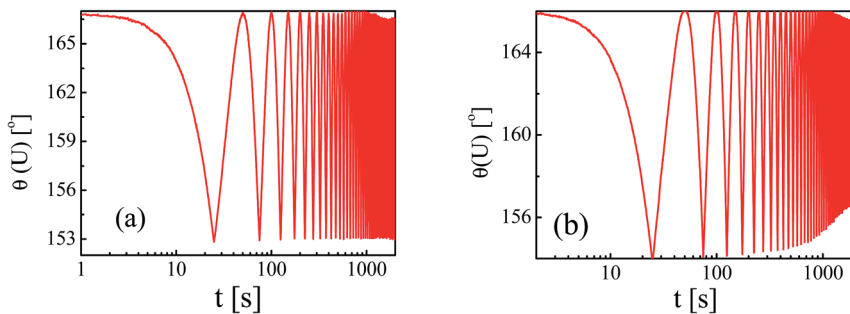
Fig. 7 EW response curves on initially pristine Teflon AF upon exposure to asymmetric voltage ramps for positive (a; $U = 0...+52$ V) and negative (b; $U = 0...-52$ V) voltage on the drop. Ramp rate: 2 V s^{-1}.
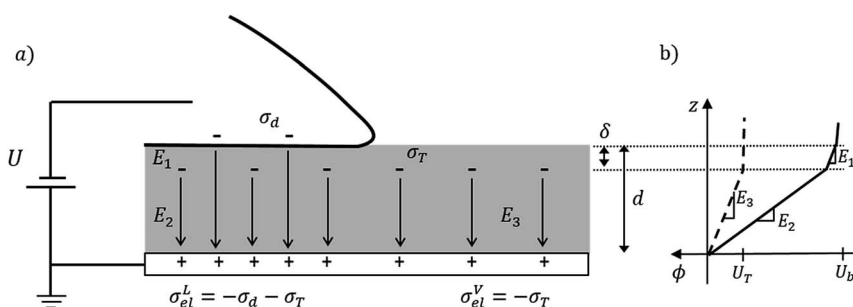

Fig. 8 (a) Schematic of the wetting drop, charge and field distribution. (b) Schematic electrostatic potential vs. distance from the electrode. Dashed line: next to the drop; solid: underneath the drop. The slopes of the potential curves in each region are given by the corresponding electric fields as indicated. (Note that the sketch is not to scale; $|\sigma_T| \ll |\sigma_d|$; $d \sim 3$ μm; δ is believed to be of molecular scale.)

for the relation between the measured value of U_T and the density σ_T of the trapped charge. A negative sign of U_T as in our experiments thus implies that σ_T is negative, too. Third, from the derivation in the appendix it becomes clear that U_T is the potential with respect to the ITO electrode of the trapped charge next to the drop. The electrostatic energy in this part of the sample thus plays the decisive role for the asymmetry of the EW response curves: no charge next to the drop implies a symmetric EW response. Finally, we note that the expression for U_T depends on the depth δ by which the trapped charge is submerged into the polymer. This depth cannot be determined from the analysis. As long as δ does not reach values close to d, however, the order of magnitude of σ_T remains unaffected.

While we make use of the model of Verheijen and Prins[29] to analyze our data, we note that the nature of the trapped charge in our experiments is very different. In that study as well as more recent work reporting similar observations, the dielectric layer consisted of a composite layer of two different materials, a primary dielectric layer such as a micrometer thick layer of another polymer (e.g. SU8, Parylene) or an inorganic dielectric layer (SiO$_2$, Al$_2$O$_3$) that was covered by a hydrophobic top coating of nanometer thickness of either a fluoropolymer layer or a silane. In those cases, it is assumed that the hydrophobic top coating would
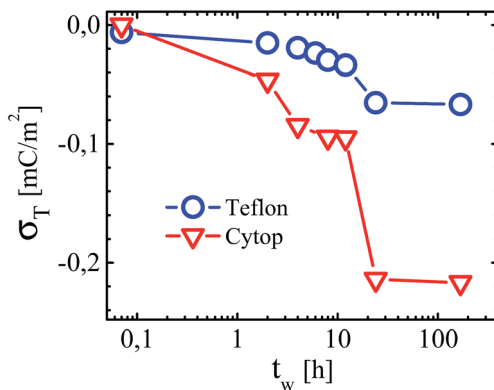
Fig. 9 Trapped charge density of Teflon AF (blue circles) and Cytop (red triangles) surface *vs.* aging time in water at pH 6, as derived from Fig. 4.

break down above a certain critical voltage and become electrically leaky in a reversible manner. Trapped charge, either positive or negative depending on the polarity of the applied voltage, is then believed to accumulate at the interface between the top coating and the primary dielectric, where it screens the electric field and induces contact angle saturation.

In contrast, the appearance of trapped charge in our experiments is not triggered by any applied voltage but generated spontaneously during aging in ambient fluid. Moreover, the voltages that we apply are well below the onset of contact angle saturation, as proven by the perfectly parabolic EW curves with a maximum contact angle reduction of merely 30° corresponding to an EW number of $\eta = \Delta\cos\theta = cU^2/2\gamma \approx 0.3$. Additionally, our EW curves are strongly asymmetric, which points to a permanent rather than reversible charging process of exclusively negative charge carriers. In fact, when testing the longevity of the trapped charge by annealing the samples, we found that annealing at 250 °C did not remove the trapped charge, see Fig. S4.†

The fact that the trapped charge is generated without applied bias voltage along with its strong increase with increasing pH, which is characteristic for many hydrophobic polymer–water interfaces,[14,19] leads us to the conclusion that the trapped charge is adsorbed directly to the polymer–water interface, or very close, by the influence of short range molecular interaction forces rather than long range electrostatic. We therefore assume that δ is of molecular scale, which implies in particular $\delta \ll d$ in eqn (3). To convert the values of U_T from Fig. 4 into trapped charge density σ_T we assume $\delta = 0$. Except for a minor correction due to the variations of d from sample to sample, the resulting plot of σ_T *vs.* aging time, Fig. 9, is very similar to Fig. 4. Note how small the absolute value of σ_T is: the average distance between adjacent charges on the surface is several tens of nanometers – much larger than, say, the size of the polymer molecules.

4. Streaming potential measurements

Complementary streaming potential measurements were carried out to characterize the nature of the charge trapped at the solid–liquid interface. From the
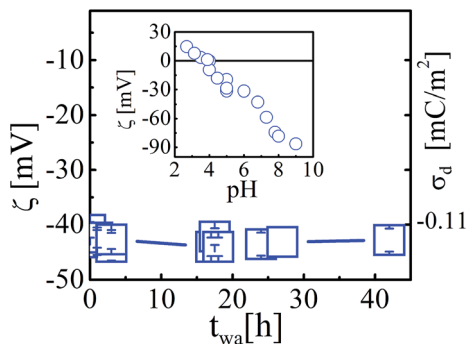
Fig. 10 ζ potential *vs.* aging time for the Teflon AF surface in de-ionized water (pH 6). Right axis: corresponding charge density of the diffuse layer as obtained from ζ potential by the Gouy–Chapman relationship. Inset: ζ potential *vs.* pH of the water at $t_w = 1$ h.

measured streaming potential we extracted a ζ potential of ≈ -40 mV for de-ionized water of unadjusted pH ≈ 6, as shown in Fig. 10. This value is consistent with the extensive literature on electrokinetic characterizations of Teflon AF–water interfaces.[14,19] Also in agreement with literature data, ζ is found to become more negative with increasing pH and found to reverse sign at the isoelectric point of Teflon at pH ≈ 3. This strong pH-dependence is the primary reason why the negative surface charge of Teflon–water interfaces is generally attributed to the adsorption of hydroxyl ions. In contrast to the trapping voltage and the trapped charge density in Fig. 9, however, the ζ potential was found to be independent of the immersion time of the surface into water. At the same time, the surface charge density as calculated from the diffuse part of the electric double layer using the value of ζ and the Gouy Chapman relation, $\sigma_d = \sqrt{8\varepsilon\varepsilon_0 RTc} \sinh(e\zeta/k_B T)$, turns out to be ≈ -0.11 mC m^{-2}, *i.e.* only slightly higher (in absolute value) than the highest values of σ_T after long term aging. (Here, R is the universal gas constant and $c \approx 10^{-6}$ mol L^{-1} is the ion concentration in the near neutral water without any added salt). Hence, the majority of the charge carriers in the electric double layer at the Teflon–water interface eventually ends up in trapped states.

5.   Discussion

Reconciliation of EW and streaming potential measurements

At first glance, the results of the EW measurements and the streaming potential measurements seem to contradict each other. While the small amount of trapped charge increases with aging time in water and has a big impact on the asymmetry of the EW response, the contribution due to adsorbed hydroxyl ions that we probe by the streaming potential measurements does not. In fact, this apparent discrepancy is caused by the fact that EW and streaming potential measurements probe different physical quantities. EW measures the variation of the interfacial energy upon spreading – streaming potential measurements quantify the density of interfacial charge that is immobilized beyond the shear plane due to interfacial adsorption. To reconcile the different aging behaviors between the two types of

measurements, we propose the existence of two different adsorption states of interfacial hydroxyl ions, the regular surface-adsorbed state that is generally used to explain the negative surface charge found in electrokinetic measurements[14,19] and an energetically deeper-lying trapped state. In both states, the hydroxyl ions are immobilized at the interface and hence their counter ions are probed by the streaming potential measurements. Thus, the latter cannot distinguish between the two different states of surface-adsorbed hydroxyl ions and only probes the sum of the two charge densities. If aging implies a gradual transformation of the immobile but reversibly bound surface-adsorbed hydroxyls into irreversibly trapped ones, the resulting ζ potential can still remain the same, as observed. In EW, however, the presence of permanently trapped ions everywhere on the surface, *i.e.* both under the drop and next to it, changes the variation of the electrostatic energy upon moving the contact line to minimize the energy (see Fig. 8). As the detailed derivation of eqn 2 in the appendix shows, this leads to the observed asymmetry of the EW response. The similarity of the charge density extracted from the ζ potential measurement and the trapped charge density suggests that a large fraction of interfacially adsorbed hydroxyl ions is eventually converted into the trapped state.

The appearance of U_T in eqn 2 implies that there is no additional charge transferred upon depositing a drop onto the surface that is kept at the potential $U = U_T$. This is consistent with the thermodynamic Lippmann equation: $\sigma = -\partial \gamma_{sw}/\partial U$. (Note that there is in part of the literature the habit to denote eqn (1) as 'Lippmann equation'. This, however, is strictly speaking incorrect. The actual equation derived and discussed by Lippmann is the relation between surface charge and interfacial tension just given. It does not involve wettability. In his studies, Lippmann always tried to ensure that the interfaces are completely water wetting. See ref. 32 and its English translation in ref. 2.)

In EW experiments on dielectric, the total charge at the fluoropolymer–water interface does not vanish at the voltage corresponding to the maximum contact angle. As discussed above, the excess charge induced by the applied voltage only amounts to a small fraction of the intrinsic charge density. One might suspect a violation of basic thermodynamics, here. This, however, is not the case. The EDL does not contribute (in a significant manner) to the energy balance of EW (on dielectric) systems. The analogue of Lippmann's equation for EW on dielectric therefore does not involve the intrinsic surface charge of the EDL but only the electrically induced excess charge between the drop and the electrode. Lippmann's equation should then be written for the effective interfacial tension $\gamma_{sw}^{eff} = \gamma_{sw} - c_d(U - U_T)^2/2$. U_T is thus the potential of zero excess charge between drop and counter electrode. It is the potential with respect to the electrode that needs to be applied to a drop such that no charge flows from the battery to the drop as it is deposited onto a water-aged substrate that carries a trapped charge density σ_T.

Microscopic interpretation of the charging process

The development of a detailed microscopic model of the charge trapping process is beyond the scope of the present work. Nevertheless, our results provide various clues pointing to important ingredients of such a model. As the density of adsorbed OH$^-$ increases with increasing pH, this increases the attempt rate and

hence the probability for some of them to stick to some trapping sites on the surface. In contrast to conventional ion adsorption processes involved in the formation of EDLs, including possible adsorption into the Stern layers, this aging process is extremely slow in the present experiments. This suggests in the first place that the charge trapping process is very different from simple adsorption to surface sites, *e.g.* on mineral–electrolyte interfaces, which can be complex[33] but usually occur in fractions of a second or faster. It is also very different from the charge injection processes reported by Thomas *et al.*[11] for composite dielectric layers composed of Cytop and silicon nitride that display a relaxation time of ≈ 50 s, the reversible trapping reported by Verheijen and Prins[29] as well as the one described by Li *et al.* on SiO_2.[28] Next to the much shorter time scales, all those experiments report a reversible injection process for both positive and negative ions, depending on the sign of the applied bias voltage. The slowness of the process in our experiments suggests that the charge trapping process is limited by kinetic barriers. This interpretation is consistent with the observation that the polarity of the applied voltage has an important impact on the charge trapping in the presence of EW (Fig. 7). In this case, the applied bias voltage could affect the adsorption kinetics by varying the barrier height rather than the attempt rate.

Two related aspects of our observation are rather remarkable: the low density of the trapped charge and the universality and stability of the phenomenon. As noted above, the characteristic values of σ_T correspond to average separations between adjacent trapped charge carriers of several tens of nanometers. The origin of this length scale is not obvious. Any reasonable estimate of a 'site density' of trap sites should relate to the structure of the material. Teflon AF and Cytop are both co-polymers of tetrafluoroethylene with different types of oxygen-containing cyclic rings. One natural assumption would be that the oxygen-containing groups on the individual polymer molecules are involved in the charging process. Interestingly, in the context of electrets – *i.e.* materials that can permanently store electric charge – the molecular properties of fluoropolymer molecules have been inferred to explain variations in charge storage capacities between different compounds of Teflon AF and Cytop.[34] As in our experiments, the charge storage capacity of fluoropolymer electrets is approximately three times higher for Cytop than for Teflon AF. In contrast to our experiments, however, charging of the electrets is conventionally carried out by bombarding the surfaces with electrons under vacuum. Interestingly, our experiments suggest that prolonged exposure to water could be an alternative method to charge fluoropolymer electret materials.

Teflon AF as well as Cytop are known to display porosity on the nanoscale of the order of 10%. This is the basis of their use for gas filtration membranes. One might therefore speculate that the low density of trapped charges reflects the spacing between nano-scale pores. The necessity of charge carriers to enter sub-nanometric pores could also explain the existence of rather high kinetic barriers and thus long equilibration times, as already suggested above. Part of that energy barrier would probably result from the breaking of hydrogen bonds upon entering such pores and another part from electrostatic interactions. For the latter, we can estimate the contribution of the external field to the bias-dependence of aging under EW (Fig. 7): for a typical electric field E of a few tens of V μm^{-1}, penetration into a pore by one nanometer to reach a suitable trapping site involves a variation of the electrostatic potential $\Delta\phi = E \times 1$ nm of

a few tens of mV – a value of the order of thermal energies. It is thus plausible that a suitable bias voltage (positive on the drop) can suppress the formation of trapped charge by increasing the energetic barrier to charge trapping. (Note that this specific choice of polarity is also used in commercial applications of EW in optofluidics lenses and displays.) The observation that Cytop displays a higher density of trapped charge than Teflon AF is consistent with the fact that Cytop is slightly more porous.

Assuming that the adsorbing species are indeed hydroxyl ions, the idea of a low site density in combination with barrier-limited trapping kinetics is also compatible with the observation of the similar spontaneous charging for the other fluids shown in Fig. 5 and in humid air. Since we did not take any precautions to specifically dry any of these fluids, it is plausible, in a barrier-limited process that residual water in the fluids finds its way to the surface and then contributes to the charging with little dependence on the bulk density. Surface-induced autolysis, as a widely suggested mechanism involved in the charging of hydrophobic surfaces[19] would then assist in generating the charge hydroxyl ions.

Finally, we note that polymer surfaces exposed to water are not necessarily static. Siretanu *et al.*[35] demonstrated that many polymer surfaces display spontaneous rearrangements of material that leads to nano-scale roughening. This phenomenon depends on the composition of the water (pH, dissolved salts) and is particularly pronounced for degassed water. It is believed to be caused by a combination of local electric fields and enhanced mobility of the polymer molecules in the immediate vicinity of the surface.[35,36] Recently, it was shown that similar nanostructures also appear in EW experiments on polystyrene surfaces.[37] Like in the case of polystyrene, AFM images of water-aged Teflon AF surfaces in the present study also display characteristic bumps of nanometer height and typical separations of a few tens of nanometers, as shown in Fig. S5.† In a more general sense, this suggests that modifications of the polymer surfaces should also be considered as a potentially important aspect in the long term stability and/ or degradation of substrate materials for EW.

6. Conclusions

This study was motivated by the experimental observation of a growing asymmetry in EW response curves on fluoropolymer surfaces after prolonged aging in water. A systematic analysis of the phenomenon and comparison to streaming potential measurements on the equally treated surfaces revealed a number of subtle aspects of the relationship between the macroscopic (electro)wettability and microscopic physical chemistry of ion adsorption at the solid–liquid interface. While the total charge density in the electric double layer has little effect on the macroscopic wettability – as is generally known – it is crucial for the generation of permanently trapped charge and thus for the EW performance of the surface. Specifically, the strong increase of both ζ potential and trapped charge with increasing pH are consistent with the general idea that adsorbing hydroxyl ions are responsible for the negative charge density of Teflon AF– and Cytop– water interfaces. Upon prolonged exposure to water, the majority of these hydroxyl ions seems to become trapped at the interface at very low densities corresponding to average separations of up to 100 nm and thereby causes the observed asymmetry of the EW response curves. Operation at low pH as well as the

consistent choice of a positive bias on the liquid phase in EW experiments with DC voltage repel these anions from the surface and thereby suppress their adverse effect on the EW performance. Overall, our experiments highlight the relevance of the often ignored microscopic properties of the EDL for the long term stability of materials in EW.

Note added in proof

After the reviewing process and during the actual Faraday Discussion meeting, we became aware of a mistake in the conversion of the value of the ζ potential into charge density, which had caused an erroneous overestimation of the charge density. Thanks to these comments, the right hand axis in Fig. 10 was corrected. As a consequence, some of the original discussion that was devoted to possible explanations of the surprisingly large difference between the electrokinetically determined charge density and the density of trapped charge became obsolete.

Appendix

In the presence of a fixed trapped charge, the electrowetting curve is asymmetric and the contact angle becomes maximum not at zero voltage but at a finite voltage U_T. The corresponding contact angle–voltage relationship is given by eqn (2). It was derived by Verheijen and Prins.[29] The derivation of this expression is in principle straightforward. Yet, it requires a careful consideration of all contributions to the electrostatic energy. The laterally homogeneous trapped charge density σ_T is assumed to be located at a fixed depth δ below the solid surface, as shown in Fig. 8. For a dielectric with a homogeneous dielectric constant ε, the basic laws of electrostatics provide relationships between the charge densities on the drop, σ_d, the trapped charge σ_T, and the charge density on the electrode both under the solid–liquid interface, σ_{el}^L, and next to the drop under the solid–vapor interface, σ_{el}^V, and the corresponding electrostatic potentials ϕ_i^j:

$$\sigma_d = \varepsilon\varepsilon_0 E_1 = -\varepsilon\varepsilon_0 \frac{\phi_T^L - \phi_d}{\delta} \tag{A1}$$

$$\sigma_T = \varepsilon\varepsilon_0(E_2 - E_1) \rightarrow \sigma_T + \sigma_d = \varepsilon\varepsilon_0 E_2 = -\varepsilon\varepsilon_0 \frac{\phi_{el} - \phi_T^L}{d - \delta} \tag{A2}$$

$$\sigma_{el} = -\varepsilon\varepsilon_0 E_2 = +\varepsilon\varepsilon_0 \frac{\phi_{el} - \phi_T^L}{d - \delta} \tag{A3}$$

$$\sigma_T = +\varepsilon\varepsilon_0 E_3 = -\varepsilon\varepsilon_0 \frac{\phi_{el} - \phi_T^V}{d - \delta} \tag{A4}$$

The equilibrium contact angle is obtained as usual by considering the virtual work upon displacing the contact line by δx towards the right and requiring the free energy to be stationary, *i.e.*

$$\delta W = \delta W_{surf} + \delta W_{el} = 0 \tag{A5}$$

where $\delta W_{surf} = (\gamma_{sl} - \gamma_{sv} + \gamma \cos \theta)\delta x$, as usual in the derivation of Young's law. Moreover,

$$\delta W_{el} = \delta W_{batt} + \delta W_{drop} \tag{A6}$$

consists of the gain of electrostatic energy upon transferring charge from the battery to the drop. Specifically, this yields

$$\delta W_{batt} = -(\phi_d - \phi_{el})\sigma_d \; \delta x = -\frac{1}{\varepsilon\varepsilon_0}(\sigma_d \; d + \sigma_T(d - \delta))\sigma_d \; \delta x \tag{A7}$$

and

$$\delta W_{drop} = \frac{\varepsilon\varepsilon_0}{2}\left\{E_1^2 \; \delta + \left(E_2^2 - E_3^2\right)(d - \delta)\right\}\delta x = \frac{1}{2\varepsilon\varepsilon_0}\left\{d\sigma_d^2 + 2 \; (d - \delta)\sigma_d\sigma_T\right\}\delta x \tag{A8}$$

For the right-hand part of the equation, we made use of a linear combination of eqn (A1)–(A3). Combining eqn (A7) and (A8), we find

$$\delta W_{el} = -\frac{d\sigma_d^2}{2\varepsilon\varepsilon_0} \; \delta x = -\frac{\varepsilon\varepsilon_0}{2d}\left(\phi_d - \phi_T^V\right)^2\delta x \tag{A9}$$

Rewriting $\phi_d - \phi_T = (\phi_d - \phi_{el}) - (\phi_T^V - \phi_{el}) = U - U_T$ and inserting into eqn (A5), we recover eqn (2). The latter expression should be read as a definition of the trapping voltage $U_T = \phi_T^V - \phi_{el}$.

According to eqn (A4), a positive trapped charge density σ_T implies a positive voltage U_T and hence requires a positive voltage $U = U_T$ on the drop (with respect to the electrode on the substrate) to achieve the maximum contact angle. Similarly, a negative trapped charge requires a negative applied voltage. This result may seem counterintuitive at first glance. Yet, eqn (A9) implies that the electric contribution vanishes if the potential of the drop equals the potential of the trapped charge. In this case, the E_1 vanishes (see Fig. 8) and the wetting state of the drop is not affected by the externally applied voltage. Consequently, we find $\theta(U = U_T) = \theta_Y$. Note that this entire analysis does not take into account the spontaneously generated charge density due to the chemical interactions at the solid–liquid interface.

Acknowledgements

References

1 P. R. Resnick and W. H. Buck, Teflon AF Amorphous Fluoropolymers, in *Modern Fluoropolymers*, ed. J. Scheirs, Wiley, New York, 1997.
2 F. Mugele and J. C. Baret, Electrowetting: from basics to applications, *J. Phys.: Condens. Matter*, 2005, **17**(28), R705–R774.

3 S. Chevalliot, S. Kuiper and J. Heikenfeld, Experimental Validation of the Invariance of Electrowetting Contact Angle Saturation, *J. Adhes. Sci. Technol.*, 2012, **26**(12–17), 1909–1930.

4 F. Mugele, Fundamental challenges in electrowetting: from equilibrium shapes to contact angle saturation and drop dynamics, *Soft Matter*, 2009, **5**(18), 3377–3384.

5 A. Quinn, R. Sedev and J. Ralston, Influence of the electrical double layer in electrowetting, *J. Phys. Chem. B*, 2003, **107**(5), 1163–1169.

6 E. Seyrat and R. A. Hayes, Amorphous fluoropolymers as insulators for reversible low-voltage electrowetting, *J. Appl. Phys.*, 2001, **90**(3), 1383–1386.

7 H. Moon, *et al.*, Low voltage electrowetting-on-dielectric, *J. Appl. Phys.*, 2002, **92**(7), 4080–4087.

8 B. Janocha, *et al.*, Competitive electrowetting of polymer surfaces by water and decane, *Langmuir*, 2000, **16**(7), 3349–3354.

9 S. Berry, J. Kedzierski and B. Abedian, Irreversible electrowetting on thin fluoropolymer films, *Langmuir*, 2007, **23**(24), 12429–12435.

10 S. Berry, J. Kedzierski and B. Abedian, Low voltage electrowetting using thin fluoroploymer films, *J. Colloid Interface Sci.*, 2006, **303**(2), 517–524.

11 D. Thomas, *et al.*, Charge injection in dielectric films during electrowetting actuation under direct current voltage, *Thin Solid Films*, 2015, **590**, 224–229.

12 B. Raj, *et al.*, Ion and Liquid Dependent Dielectric Failure in Electrowetting Systems, *Langmuir*, 2009, **25**(20), 12387–12392.

13 C. D. Daub, D. Bratko and A. Luzar, Electric Control of Wetting by Salty Nanodrops: Molecular Dynamics Simulations, *J. Phys. Chem. C*, 2011, **115**(45), 22393–22399.

14 R. Zimmermann, *et al.*, Hydroxide and hydronium ion adsorption – a survey, *Curr. Opin. Colloid Interface Sci.*, 2010, **15**(3), 196–202.

15 J. K. Beattie, The intrinsic charge on hydrophobic microfluidic substrates, *Lab Chip*, 2006, **6**(11), 1409–1411.

16 U. Sivan, The inevitable accumulation of large ions and neutral molecules near hydrophobic surfaces and small ions near hydrophilic ones, *Curr. Opin. Colloid Interface Sci.*, 2016, **22**, 1–7.

17 D. Chandler, Interfaces and the driving force of hydrophobic assembly, *Nature*, 2005, **437**(29), 640.

18 J. K. Beattie, A. N. Djerdjev and G. G. Warr, The surface of neat water is basic, *Faraday Discuss.*, 2009, **141**, 31–39.

19 J. Lutzenkirchen, T. Preocanin and N. Kallay, A macroscopic water structure based model for describing charging phenomena at inert hydrophobic surfaces in aqueous electrolyte solutions, *Phys. Chem. Chem. Phys.*, 2008, **10**(32), 4946–4955.

20 C. S. Tian and Y. R. Shen, Structure and charging of hydrophobic material/water interfaces studied by phase-sensitive sum-frequency vibrational spectroscopy, *Proc. Natl. Acad. Sci. U. S. A.*, 2009, **106**(36), 15148–15153.

21 D. Horinek and R. R. Netz, Specific ion adsorption at hydrophobic solid surfaces, *Phys. Rev. Lett.*, 2007, **99**(22), 226104.

22 R. Vacha, *et al.*, The Orientation and Charge of Water at the Hydrophobic Oil Droplet–Water Interface, *J. Am. Chem. Soc.*, 2011, **133**(26), 10204–10210.

23 D. Choi, *et al.*, Spontaneous electrical charging of droplets by conventional pipetting, *Sci. Rep.*, 2013, **3**, 2037.

24 J. K. Moon, *et al.*, Electrical power generation by mechanically modulating electrical double layers, *Nat. Commun.*, 2013, **4**, 1487.

25 J. K. Moon, M. W. Song and H. K. Pak, Investigation of surface charge density on solid–liquid interfaces by modulating the electrical double layer, *J. Phys.: Condens. Matter*, 2015, **27**(19), 194102.

26 D. J. Lomax, *et al.*, Ultra-low voltage electrowetting using graphite surfaces, *Soft Matter*, 2016, **12**(42), 8798–8804.

27 F. Mugele, *et al.*, Ion adsorption-induced wetting transition in oil–water–mineral systems, *Sci. Rep.*, 2015, **5**, 10519.

28 X. M. Li, *et al.*, Decreasing the Saturated Contact Angle in Electrowetting-on-Dielectrics by Controlling the Charge Trapping at Liquid–Solid Interfaces, *Adv. Funct. Mater.*, 2016, **26**(18), 2994–3002.

29 H. J. J. Verheijen and M. W. J. Prins, Reversible electrowetting and trapping of charge: model and experiments, *Langmuir*, 1999, **15**(20), 6616–6620.

30 A. G. Banpurkar, K. P. Nichols and F. Mugele, Electrowetting-based microdrop tensiometer, *Langmuir*, 2008, **24**(19), 10549–10551.

31 A. Sze, *et al.*, Zeta-potential measurement using the Smoluchowski equation and the slope of the current–time relationship in electroosmotic flow, *J. Colloid Interface Sci.*, 2003, **261**(2), 402–410.

32 G. Lippmann, Relations entre les phénomènes électriques et capillaires, *Ann. Chim. Phys.*, 1875, **5**, 494–549.

33 I. Siretanu, *et al.*, Direct observation of ionic structure at solid–liquid interfaces: a deep look into the Stern layer, *Sci. Rep.*, 2014, **4**, 4956.

34 Y. Sakane, Y. Suzuki and N. Kasagi, The development of a high-performance perfluorinated polymer electret and its application to micro power generation, *J. Micromech. Microeng.*, 2008, **18**(10), 104011.

35 I. Siretanu, J. P. Chapel and C. Drummond, Water-Ions Induced Nanostructuration of Hydrophobic Polymer Surfaces, *ACS Nano*, 2011, **5**(4), 2939–2947.

36 I. Siretanu, *et al.*, Spatial Heterogeneity of Glassy Polymer Films, *Macromolecules*, 2015, **48**(8), 2787–2792.

37 Y. B. Sawane, *et al.*, Electrolyte concentration effects on DC voltage electrowetting, *Sens. Actuators, A*, 2016, **240**, 126–130.